Theoretical investigation of the effect of a magnetic field on the Landau-level structure of a modulation-doped single heterojunction having two occupied subbands

Kyu-Seok Lee and El-Hang Lee
Electronics and Telecommunications Research Institute, Taejon, 305-600 Korea
(Received 5 December 1994)

We have theoretically investigated the effects of a magnetic field on the Landau-level structure of a modulation-doped GaAs/(Al,Ga)As single heterojunction having two occupied subbands at zero field. Self-consistent calculations show that the population of the second subband and the energy gap between a Landau level of the second subband and another from the first subband reveal nearly periodic oscillations in the inverse magnetic field. The effect of population oscillations is important for the analysis of magnetotransport data or magnetoluminescence spectra from these structures.

I. INTRODUCTION

In the past several years a considerable amount of experimental and theoretical effort has been devoted to the investigation of electronic properties of a two-dimensional electron gas (2DEG) in modulation-doped single heterojunctions (MDSH's). GaAs/(Al,Ga)As MDSH's with only one occupied subband, in particular, have often been given the most attention, because these structures can attain high mobility property by suppressed scattering at higher subbands. However, in monitoring the signature of a 2DEG, optical techniques such as photoluminescence utilizing interband transition have suffered a fundamental disadvantage that the oscillator strength of the interband transitions is small compared to those of bulk excitons.[1,2] This is because a large portion in the wave function of a 2DEG in the growth direction is spatially separated from that of a photogenerated hole in the deep buffer layer.

On the other hand, in a MDSH having two occupied subbands at zero-magnetic field ($B=0$), the overlap between a 2DEG in the second subband (E_2) and a photogenerated hole can be made large enough so that the PL peaks associated with this transition can be readily distinguished from other emission peaks from the bulk. Recently, the magnetophotoluminescence of MDSH's having two occupied subbands showed pronounced oscillations in the luminescence intensity of the hybridized exciton recombination, as well as in its peak energy and peak width.[3] Oscillations in the luminescence intensity was explained by the combination of population effects of E_2 and a many-body interaction[4-8] between the E_2 exciton and the Fermi edge resonance[9,10] of Landau levels from the first subband (E_1). The many-body interaction, known as the optical Shubnikov–de Haas (OSdH) effect[11] was found to be largest when the Fermi level lies within the extended states, i.e., at odd-integer filling factors.

However, it should be noted that the population of E_2 in a 2DEG system with two occupied subbands at $B=0$ is sensitively dependent on B fields. The potential energy of a 2DEG at the heterojunction is sensitive to the change in the spatial density distribution of a 2DEG. This means that the effect of oscillations in the population of E_2 on the Landau-level structure of a MDSH structure is considerable. Therefore, it is important to consider this effect in the analysis of magnetotransport data, such as Shubnikov–de Haas (SdH) oscillations. This effect must be taken into account before oscillations in optical spectra can be ascribed to oscillations in many-body interactions. Though a qualitative discussion on this effect was addressed by Skolnick, Simmonds, and Fisher[12] no rigorous calculations for population effects of E_2 on the Landau-level structure of MDSH's have been reported even to date, to the best of our knowledge.

In this work, therefore, focusing on the effect of population in E_2, we investigate the B-field dependence of Landau levels in a MDSH, with two populated subbands at $B=0$. A schematic subband structure of a MDSH is plotted in Fig. 1. The paper is organized as follows. The

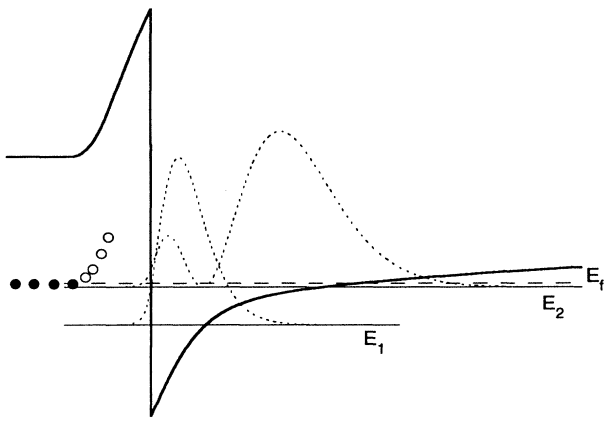

FIG. 1. A schematic subband structure of MDSH with two occupied subband at $B=0$. The open and closed circles represent ionized and neutral donors, respectively. The thick solid line, the thin solid lines, the dotted curves, and the dashed line denote the potential profile, subband energies, the squared wave functions of two subbands, and the Fermi level, respectively.

0163-1829/95/51(19)/13315(5)/$06.00

theoretical framework is detailed in Sec. II. For Landau-level structure, we consider a self-consistent numerical method, which takes into account many-body effects including the Hartree and exchange-correlation potentials. A few selected results of a model GaAs/(Al,Ga)As MDSH are presented and discussed in Sec. III, followed by a summary in Sec. IV.

II. FORMALISM

In our formalism, we consider the effects of E_2 population on Landau-level structure of a MDSH with two occupied subbands at $B=0$, and take the following assumptions: (i) the dispersion of the conduction band is parabolic so that the effective mass of an electron is independent of its energy and wave vector, and (ii) both the electronic g factor of a 2DEG and the total carrier density are independent of the B field. These assumptions may not represent a real semiconductor heterojunction, but simplify both the formalism and calculation without a considerable modification of a real system. The temperature of a 2DEG is set to be $T=0$ K for further simplicity.

In the effective mass approximation, the envelope function of electron states in the presence of a B field applied in the direction parallel to the growth axis, $\mathbf{B}=B\hat{z}$, may be represented by the solution to the following Schrödinger equation:

$$\left\{\frac{1}{2m^*}[\mathbf{p}+e\,\mathbf{A}(\mathbf{r})]^2+V_{\rm qw}(z)+V_H(z,B)+V_{\rm xc}(z,B)+sg^*\mu_B B-E\right\}\psi(\mathbf{r})=0\ , \quad (1)$$

where $\mathbf{r}=(x,y,z)$ is the position vector, $\mathbf{A}(\mathbf{r})=-\mathbf{r}\times\mathbf{B}/2$ is the vector potential, $m^*(z)$ is the effective mass of an electron, $s=\pm\frac{1}{2}$ denotes spin-up/down states, and e, g^*, and μ_B are the absolute electronic charge, the electronic g factor in the 2D channel, and the Bohr magneton, respectively. The effective mass of an electron, $m^*(z)$ and the quantum-well potential, $V_{\rm qw}$, are assumed to change abruptly at the interface between well and barrier layers. V_H and $H_{\rm xc}$ are the Hartree potential and the exchange-correlation potential, respectively, and depend implicitly on the B field as the population of each subband is dependent on the B field. V_H satisfies the Poisson's equation,

$$\frac{d^2}{dz^2}V_H(z)=\frac{e^2}{\epsilon\kappa}[\rho_d(z)-\rho_e(z)-\rho_a(z)]\ , \quad (2)$$

where ρ_d is the density of ionized donors in the barrier layer, and ρ_a and ρ_e are those of ionized acceptors and free electrons in the 2D channel, respectively. The dielectric constant κ is assumed to be the same in both the barrier layer and the 2DEG channel. $V_{\rm xc}(z)$ can be formulated using the local-density-functional approximation. We use the following parametrized formula introduced by Hedin and Lundqvist,[13]

$$V_{\rm xc}(z)=-\frac{2}{\pi\alpha r_s(z)}[1+0.7734x\ln(1+x^{-1})]\mathcal{R}_y^*\ , \quad (3)$$

where $\alpha=(4/9\pi)^{1/3}$, and $x=r_s(z)/21$. $r_s(z)$ is the radius of a sphere containing an electron, and is defined in the unit of the effective Bohr radius a^* as follows:

$$r_s=[\tfrac{4}{3}\pi a^{*3}\rho_e(z)]^{-1/3}\ ,\quad a^*=\frac{4\pi\epsilon_0\kappa\hbar^2}{m^*e^2}\ .$$

$\mathcal{R}_y^*=e^2/8\pi\epsilon_0\kappa a^*$ is the effective Rydberg constant of electron in the 2DEG channel. Stern and Sarma[14] also used Eq. (3) for the calculation of energy levels in GaAs/(Al,Ga)As heterojunctions.

The energies of Landau levels for $k=0,1,2\ldots$ from the ith subband ($i=1,2$) may be written by the following form:

$$E_{i,k,s}(B)=E_i(B)+\frac{\hbar eB}{m^*}(2k+1)+sg^*\mu_B B\ , \quad (4)$$

where $E_i(B)$ represents the effective subband edge in the presence of a B field and satisfies the following one-dimensional Schrödinger equation:

$$\left[-\frac{\hbar^2}{2}\frac{\partial}{\partial z}\frac{1}{m^*(z)}\frac{\partial}{\partial z}+V_{\rm qw}(z)+V_H(z,B)+V_{\rm xc}(z,B)\right]\phi_i(z)=E_i(B)\phi_i(z)\ . \quad (5)$$

We use boundary conditions that the amplitude of $\phi(z)$ and $(1/m^*)(\partial/\partial z)\phi(z)$ are continuous at the heterointerface. V_H and $V_{\rm xc}$ are calculated from Eqs. (2) and (3) after the density of a 2DEG is obtained by

$$\rho_e(z)=\sum_i N_i|\phi_i(z)|^2\ . \quad (6)$$

At $T=0$ K, N_i, the areal density of electrons at E_i, is given by

$$N_i=\begin{cases}\dfrac{m^*}{\pi\hbar^2}(E_f-E_i)\theta(E_f-E_i) & \text{for } B=0;\\ \displaystyle\sum_{k,s}\frac{Be}{h}\theta(E_f-E_{i,k,s}) & \text{for } B\neq 0\ ,\end{cases} \quad (7)$$

where E_f denotes the Fermi energy of a 2DEG, and $\theta(x)$ is 1 for $x>0$, 0 for $x<0$, and for $x=0$ a real number between 0 and 1, to be determined from the condition that $N_e=\sum N_i$.

In the numerical calculations, first, we determine the total electron density, $N_e=\sum_i N_i(B=0)$, confined at the heterojunction at $B=0$, by self-consistent numerical procedures using Eqs. (2), (5), (6), and (7). For a MDSH with two occupied subbands at zero field, we carry out a series of calculations for $E_1(B)$ and $E_2(B)$, using Eqs. (5) and (6) as a function of $N_2(=N_e-N_1)$ for $0\le N_2<N_e/2$. With (N_1,N_2) and (E_1,E_2), we finally calculate B-field values satisfying the condition that a set of (N_1,N_2) calculated from Eqs. (4) and (7) is equivalent to the given set in the previous step.

III. RESULTS AND DISCUSSION

We consider a model MDSH that consists of a thick, nominally undoped GaAs buffer layer, followed by an undoped $Al_{0.35}Ga_{0.65}As$ spacer layer with a width of 6 nm, a thick, Si-doped $Al_{0.35}Ga_{0.65}As$ layer and, finally, a GaAs cap layer. Donor impurities at a density of 2.0×10^{18} cm^{-3} are uniformly doped in the barrier layer, except in the region of a spacer, and electrons are released from the donor impurities to the two-dimensional (2D) channel of the GaAs layer. The barrier height and the ionization energy of a Si-donor in the barrier layer is chosen to be 305 and 100 meV,[14] respectively. The effective mass of electron in the well and the barrier layer is given by $0.0665m_e$ and $0.0957m_e$, respectively. We use the same values of dielectric constant $\kappa=12.58$ and the g factor $g^*=-0.44$ for both GaAs (Ref. 15) and (Al,Ga)As.

Figure 2 displays $\Delta E(B)\equiv E_2(B)-E_1(B)$ as a function of N_2 for four different densities of electron gases at $N_e=8.8$, 9.0, 9.2, and 9.4×10^{11} cm^{-2} with ionized donors at an areal density of $N_d=9.4\times10^{11}$ cm^{-2} and ionized acceptors at $N_a=N_d-N_e$. The dashed line on + symbols represents the calculated results of $\Delta E(B=0)$, while the solid lines represent those for given N_e in various B fields applied in the direction parallel to the growth axis. For a given N_e, $\Delta E(B)$ increases monotonically as N_2 increases. As more electrons are occupied in E_2, the electric-field strength in the 2D channel increases, and so does $\Delta E(B)$. The upper limit of each solid line represents the maximum population in E_2. The dotted line is an interpolation between two data at $N_2=0$ and 2.3×10^{10} cm^{-2}, below which a confined state of E_2 was not found by our numerical algorithm. $\Delta E(N_2=0)$ was obtained from the difference between the flat band edge in the bulk GaAs layer and the calculated E_1. As N_e increases, $\Delta E(B=0)$ and $\Delta E(N_2=0)$ decrease, because the confinement effect of the potential energy is reduced as the density of ionized acceptors decreases to increase N_e. For $B=0$, the calculated results show that this effect is stronger than the contrary effect from an increase in N_2.

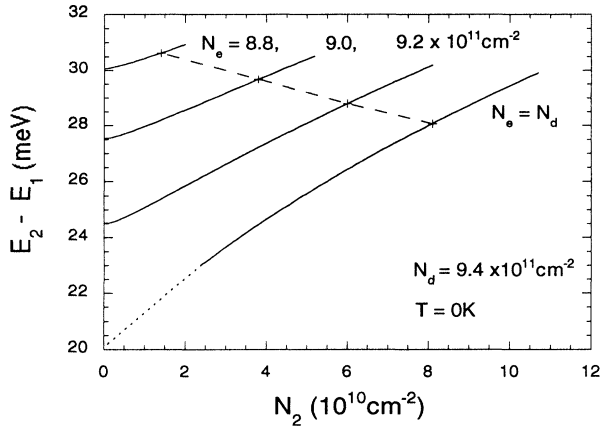

FIG. 2. Calculated gap energy $\Delta E(B)=E_2(B)-E_1(B)$ as a function of the population of the second subband at temperature $T=0$ K. The dashed line on + symbols represents the calculated results in either N_2 or N_e at $B=0$, while the solid lines are those obtained at arbitrary strengths of a magnetic field for $N_e=8.8$, 9.0, 9.2, and 9.4×10^{11} cm^{-2}. The density of ionized donors is 9.4×10^{11} cm^{-2}, while the density of ionized acceptors is determined from $N_a=N_d-N_e$.

To show the dependence of N_e on the B field, the calculated results for the case of $N_d=9.4\times10^{11}$ cm^{-2} and $N_e=9.2\times10^{11}$ cm^{-2} are plotted in Fig. 3. It is seen that the population in E_2 oscillates in a nearly periodic manner as a function of the inverse magnetic field. The oscillations of the N_2 develop discrete group oscillations as E_f moves from a Landau level at E_2 to the next Landau level in the same subband. A node is made between two oscillation groups at the B field, where the oscillating E_f is effectively in the midgap of two Landau levels of E_2, which will be shown in Fig. 4. The inset in Fig. 3 displays a plot in an expanded scale in high B fields. It is clearly seen that the oscillation period is larger then two units of the filling factor, $\nu=N_eh/eB$. For this MDSH model, the second subband is depopulated in a finite region of magnetic field starting from $\nu=6$ and 4 from the larger values. For $\nu<2$, the second subband is depopulated. In this plot, spin splittings in the population oscillations are barely discernible in the oscillation peaks for $\nu>4$, because the g factor of GaAs is relatively small.

In Fig. 4, we display the calculated Landau levels as a function of the B field for the same MDSH structure as plotted in Fig. 3. With this figure, we choose the reference energy in such a way that the Landau levels of E_2 are linear in energy and have the zero offset at $B=0$. With this choice, the slopes of Landau levels of E_1 are changed when they cross a Landau level of E_2 where E_f resides. It is noted that the three levels have the same energies for a certain region of B fields, where electrons in two Landau levels can exchange electrons, while keeping E_f frozen to them. This peculiar property is due to the sensitive response of potential energy of MDSH's to the change of N_2. In other words, when a Landau level from E_1 passes the Fermi level by giving up electrons to other

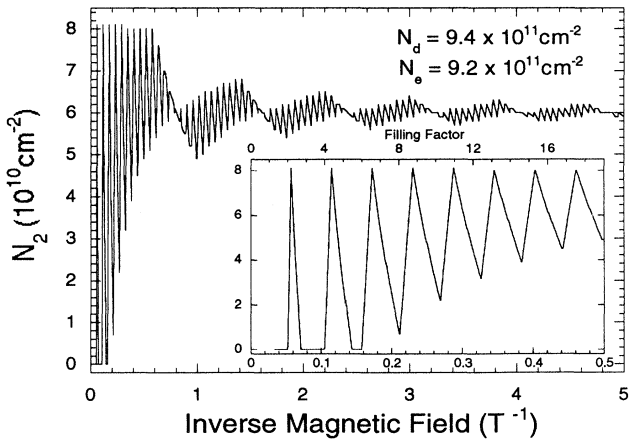

FIG. 3. Calculated N_2 as a function of $1/B$ for a MDSH with $N_e=9.2\times10^{11}$ cm^{-2} and $N_d=9.4\times10^{11}$ cm^{-2}. The inset is a close-up plot of the high B-field data.

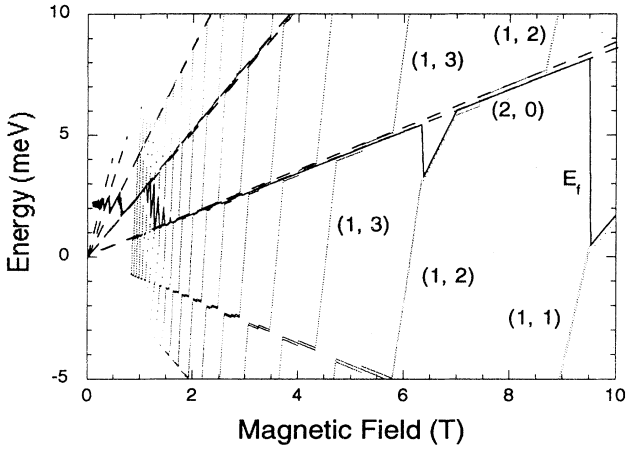

FIG. 4. Landau levels and the Fermi level of the MDSH as was calculated in Fig. 3. Landau levels from $i=1$, 2 subbands and the Fermi levels are plotted by the dotted, dashed, and solid lines, respectively. (i,k) with $k=0,1,2\ldots$ denotes the kth Landau level from the ith subbands. The reference energy is chosen such that E_2 Landau levels are linear and have zero offsets at $B=0$.

levels, the rate of this process as a function of ΔB, the increase in the magnetic field, has a certain limit, beyond which ΔE can be larger than $2\hbar e\Delta B(k_2-k_1)/m^*+(s_2-s_1)g^*\mu_B\Delta B$, the energy difference of two Landau levels from E_2 and E_1. The first subband Landau level has its energy pinned at the Fermi energy when the above two terms are balanced to be the same at a certain rate of depopulation in this Landau level. In the inset of Fig. 3, this B-field region is located at the right-hand side of each oscillation peak. From Figs. 3 and 4, we find that the population of E_2 shows a local maximum when a Landau level of E_1 leaves E_f to the higher energy side, i.e., at even integers of $\nu_1=N_1h/eB$, which is associated with the filling factor of Landau levels from E_1. However, it should be noted that ν_1 is not isomorphic with B, as N_1 is an oscillating function of B fields.

It is worth discussing some effects of the population of E_2 that can be revealed in SdH oscillations. Low-frequency oscillations may be visible at low B fields when ν_1 is too large for the SdH oscillations for E_1 to be resolved. As the amplitude of N_2 oscillations in this region is small, the periodicity of oscillations measures N_2 with a small deviation. In higher B fields, the following two cases are considered. First, when E_f is in the region between two Landau levels of E_2, i.e., $E_{2,k}<E_f<E_{2,k+1}$, the contribution of a filled Landau level in E_2 to the density of states is the same as that of a filled Landau level from E_1. Therefore, the periodicity of SdH oscillations are associated with ν and measures N_e. In this region, local maxima of SdH oscillations may occur at odd filling factors of ν.[16] Second, if E_f resides in a Landau level of E_2, the probability of elastic scattering can be maximized when all the fermi electrons fill this level, but depopulate the other level with the same energy from E_1, and vice versa. Therefore, the maxima of SdH oscillations may occur at integers of ν_1 at both ends of an interval where E_f, one Landau level from E_1, and another from E_2 have the same energy. For MDSH's with a small $N_2(B=0)$, the two maxima of SdH oscillations at both ends of each interval merges into one peak. From the inset in Fig. 3, it is seen that in high B fields all the maxima of N_2 reveal nearly the same value, slightly larger than $N_2(B=0)$ at even integers of ν_1. This implies that N_1 can be determined experimentally from the linear relation of $1/B$ to even integers of ν_1 at the maxima of N_2 oscillations, but the value of N_2 determined in this way may be slightly smaller than $N_1(B=0)$.

On the other hand, magneto-oscillations in luminescence energy can be observed from a MDSH with a large N_2 at $B=0$, because the variation of the $\Delta E(B)$ increases as N_e increases, as was shown in Figs. 2 and 4. In the presence of a photogenerated hole, the probability of the recombination of a 2DEG in E_2 with this hole will be proportional to N_2, if the hybridized excitonic effect is not taken into account. In this approximation, oscillations of luminescence intensity show an oscillatory behavior that is similar to that of the E_2 population and are nearly periodic in $1/B$. Luminescence peaks occur when a Landau level of E_1 is depopulated above E_f, i.e., at integer filling factors of N_1. It is noted that many-body interactions such as the Fermi-edge singularity in optical spectra,[12] population-dependent exchange enhancement of the g factor,[17] and the coupling of E_2 exciton with the Fermi sea[4-8] need to be considered for an analysis of the luminescence spectra of MDSH's with two occupied subbands. The consideration of these effects will be the subject of further study.

IV. CONCLUSION

In summary, we have carried out self-consistent calculations for the Landau-level structure of MDSH's with two occupied subbands at $B=0$. Both the population of E_2 and the energy gap between Landau levels from E_2 and E_1 show nearly periodic oscillations in $1/B$. Magneto-oscillations in the population of E_2 result from the crossing of Landau levels from E_1 with those of E_2. Positions of these maxima are related with the filling factor of N_1, but not with integer filling factors of N_e. When a Landau level from E_1 crosses another level of E_2 where E_f resides, their energies remain equal with each other for a finite region of magnetic field. This phenomenon results from a sensitive response of the potential energy of a MDSH to the variation in the distribution of 2DEG. In this paper, it was emphasized that the effect of population oscillations must be accounted for an interpretation of both magnetotransport data and magnetoluminescence spectra of MDSH's with two occupied subbands at $B=0$, before other many-body interactions are introduced.

ACKNOWLEDGMENTS

We would like to thank Dr. Sam Kyu Noh and Ju In Lee for helpful discussions related on the subject of this paper. This work has been funded by Korea Telecom and the ministry of Communications, Korea.

[1]C. H. Yang, S. A. Lyon, and C. W. Tu, Superlatt. Microstruct. **3**, 269 (1987).
[2]Emil S. Koteles, J. Y. Chi, and R. P. Holmstrom, Proc. SPIE **794**, 61 (1987).
[3]F.A. J. M. Drissen, S. M. Olsthoorn, T. T. J. M. Berendschot, H. F. Pen, L. J. Gilling, G. A. C. Jones, D. A. Ritchie, and J. E. F. Forst, Phys. Rev. B **45**, 11 823 (1992).
[4]T. Uenoyama and L. J. Sham, Phys. Rev. Lett. **65**, 1048 (1990).
[5]J. F. Mueller, Phys. Rev. B **42**, 11 189 (1990).
[6]I. E. Perakis and Y.-C. Chang, Phys. Rev. B **43**, 12 556 (1991).
[7]P. Hawrylak, Phys. Rev. B **44**, 11 236 (1991).
[8]G. E. W. Bauer, Phys. Rev. B **45**, 9153 (1992).
[9]G. D. Mahan, Phys. Rev. **153**, 882 (1967).
[10]M. S. Skolnick, J. M. Rorison, K. J. Nash, D. J. Mowbray, P. R. Tapster, S. J. Bass, and A. D. Pitt, Phys. Rev. Lett. **58**, 2130 (1987).
[11]W. Chen, M. Fritze, A. V. Nurmikko, D. Ackley, C. Colvard, and H. Lee, Phys. Rev. Lett. **64**, 2434 (1990).
[12]M. S. Skolnick, P. E. Simmonds, and T. A. Fisher, Phys. Rev. Lett. **66**, 963 (1991).
[13]L. Hedin and B. I. Lundqvist, J. Phys. C **4**, 2064 (1971).
[14]F. Stern and S. D. Sarma, Phys. Rev. B **30**, 840 (1984).
[15]C. Hermann and C. Weishbuch, Phys. Rev. B **15**, 823 (1977).
[16]J. C. Portal, R. J. Nicholas, M. A. Brummell, A. Y. Cho, K. Y. Cheng, and T. P. Pearsall, Solid State Commun. **43**, 907 (1977).
[17]R. J. Nicholas, R. J. Haug, K. v. Klitzing, and G. Weimann, Phys. Rev. B **37**, 1294 (1988).